ELSEVIER

Journal of Organometallic Chemistry 566 (1998) 61–71

Journal of Organometallic Chemistry

Palladium(II) allyl complexes with nitrogen–sulfur bidentate ligands. Substituent effects in the mechanism of allyl amination

Luciano Canovese *, Fabiano Visentin, Paolo Uguagliati, Gavino Chessa, Andrea Pesce

Dipartimento di Chimica, Universita' di Venezia, Calle Larga Santa Marta, 2137-30123 Venezia, Italy

Received 21 January 1998; received in revised form 13 May 1998

Abstract

The reactivity of palladium(II) allyl complexes containing the nitrogen–sulfur bidentate ligand N–SR (N–SR = 2-(phenylthiomethyl)pyridine, 2-(phenylthiomethyl)-6-methylpyridine, 2-(*tert*-butylthiomethyl)pyridine) was studied in $CHCl_3$ in the presence of the activated olefin fumaronitrile (fn). The stepwise mechanism involves a fast pre-equilibrium in which the N–SR ligand is displaced by the amine with formation of an inert bis-amino allyl species and concomitant rate-determining bimolecular attack of the amine on the coordinated allyl moiety to give the allylamine and the olefin-stabilized Pd(0) complexes [Pd(η^2-fn)(N–SR)]. The influence of the substituents at the allyl fragment and at the nitrogen–sulfur ligand is rationalized together with the fluxional behavior in solution.

1. Introduction

We have been carrying out a systematic mechanistic investigation of the nucleophilic attack by amines at the allyl group in Pd(II) η^3-allyl complexes bearing bidentate ligands such as α-diimines [1] or 2-pyridylthioethers (L–L′) [2] in the presence of activated olefins (ol) leading to Pd(0) olefin complexes [Pd(η^2-ol)(L–L′)] and allylamines. Nucleophilic attacks at coordinated allyl groups are of great interest for their potential applications in the field of metal catalyzed organic synthesis [3]. We showed that the reaction proceeds via fast equilibrium displacement of L–L′ to yield an inert bis-amino species accompanied by a rate-determining nucleophilic attack at the allyl ligand leading to the Pd(0) olefin complex and allylamine. Quite recently attention has been focused on the factors affecting the steric and electronic control of the regio- and stereo-selectivity of nucleophilic attack at the allyl group, such as the bulkiness of the bidentate ligand and the presence of different ligating atoms [4]. In this context studies have involved mixed chelating ligands containing P,N [5], P,O [6], P,S [7] and N,S [8].

We have now extended our previous mechanistic study on Pd(II) η^3-allyl complexes of the N,S ligand C_5H_4N-2-CH_2SR (N–SR) [2] to include the steric and electronic effects brought about by substituents at both the allyl group and the sulfur on the rate of amination and on the extent of bidentate ligand equlibrium displacement. To this end we describe herein the mechanism of reaction of piperidine, diethylamine, and morpholine with the complexes [Pd(η^3-substituted allyl)(N–SR)]$^+$ in $CHCl_3$ in the presence of fumaronitrile (fn).

2. Results and discussion

The N–S chelate η^3-allyl complexes [Pd(η^3-all)(N–SR]ClO_4 [(**1**); N–SR=C_5H_4N-2-CH_2SR, R = Ph, *t*-Bu; 6-MeC_5H_3N-2-CH_2SPh; all = C_3H_5, 2-MeC_3H_4, 1,1-$Me_2C_3H_3$] were prepared by addition of the N–S ligand to [Pd(η^3-all)Cl]$_2$ in CH_2Cl_2. They react smoothly with the amines piperidine (Pip), diethylamine (Dea), morpholine (Morph) (HY) in $CHCl_3$ at 25°C in the pres-

* Corresponding author. Tel.: +39 41 2578571; fax: +39 41 2578517.

0022-328X/98/$19.00
PII S0022-328X(98)00715-3

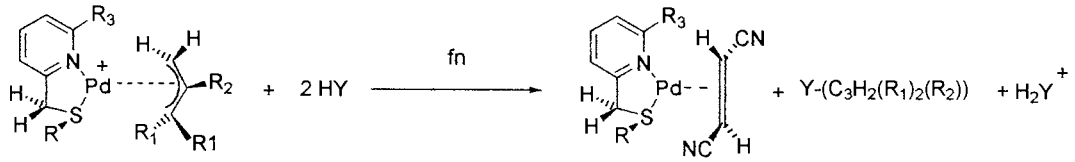

1 2 3

R = Ph ; R_1 ,R_2 = H ; R_3 = H (1a)

R = Ph; R_1 = H ; R_2 = Me ; R_3 = H; (1b)

R = Ph; R_1 = Me ; R_2 = H ; R_3 = H; (1c)

R = t-Bu ; R_1 , R_2 = H ; R_3 = H (1d)

R = t-Bu; R_1 = H ; R_2 = Me ; R_3 = H (1e)

R = t-Bu;R_1 = Me ; R_2 = H ; R_3 = H (1f)

R = Ph ; R_1 , R_2 = H ; R_3 = Me (1g)

HY = pip,dea,morph

fn = fumaronitrile

Y-C_3H_5 , Y-C_3H_4Me

3

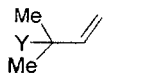

(3a)

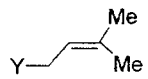

(3b)

Scheme 1.

ence of the activated olefin (fn) to give the Pd(0) olefin complexes [Pd(η^2-fn)(N–SR)] (**2**) and the allylamine Y–($C_3H_2(R_1)_2(R_2)$) (**3**) (Scheme 1).

The course of the reaction was followed by monitoring UV–VIS spectral changes in the wavelength range 250–400 nm of $CHCl_3$ solutions of **1** ($[Pd]_0$ ca. 1×10^{-4} mol dm^{-3}) in the presence of fn ($2–8 \times 10^{-4}$ mol dm^{-3}) and of an excess of N–SR ($1–20 \times 10^{-3}$ mol dm^{-3}) upon addition of variable aliquots of HY in the concentration range $1–150 \times 10^{-3}$ mol dm^{-3}. The reaction was also monitored by NMR spectrometry and its course was confirmed by the typical ^{1}H spectra of allylamine and of complex **2** (see Section 5).

Under these conditions the reaction went smoothly to completion, as indicated by comparison of solution spectra after seven to eight half lives with those of the final products prepared independently. The conversion of **1** into to **2** with time appeared to obey the mono–exponential relationship $A_t = A_\infty + (A_o - A_\infty)\exp(-k_{obs}t)$, corresponding to a pseudo-first order process

$$-d[\mathbf{1}]/dt = k_{obs}[\mathbf{1}] \quad (1)$$

The k_{obs} values, determined by non-linear regression analysis of A_t versus t data, showed a bivariate dependence on HY and N–SR concentrations (which could be viewed as constant with time, being largely in excess over the metal substrates) (Eq. 2):

$$k_{obs} = k_2[HY]/(1 + K_E\,[HY]^2/[N–SR]) \quad (2)$$

which can be re-written as

$$k_{obs}/[HY] = k_2/(1 + K_E\rho) \quad (3)$$

where $\rho = [HY]^2/[N–SR]$.

The parameters k_2 and K_E were determined by non-linear regression of rate constants to Eq. 3 (Fig. 1).

The values of k_2 and K_E are listed in Table 1. Moreover, the rate of reaction carried out at various fn concentrations in the range $2–8 \times 10^{-4}$ mol dm^{-3} proved independent of (fn), other things being equal, indicating that the activated olefin plays no role in the rate determining step.

Such a dependence which is not unprecedented [1,2] was interpreted on the basis of the stepwise mechanism shown in Scheme 2.

According to this mechanistic picture, the η^3-allyl substrate **1** is in fast pre-equilibrium with the inert bis-amino species **4** via displacement of the bidentate ligand N–SR. It also undergoes concomitant rate determining bimolecular attack by the amine (k_2 step) to give a labile Pd(0) intermediate **I** bearing an η^2-bound

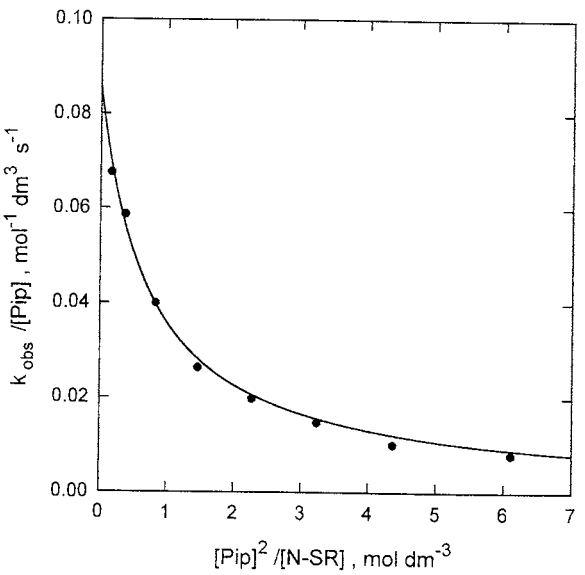

Fig. 1. Dependence of k_{obs}/[Pip] on [Pip]^2/[N–SR], (R = *t*-Bu) for reaction of **1e** with piperidine at 25°C.

allyl cation which is rapidly and quantitatively displaced by the activated olefin fn to give the final product **2**. The reliability of the mechanism in Scheme 2 was independently proved by ^{1}H-NMR experiments carried out in $CDCl_3$ or CD_2Cl_2 in which an excess of amine was added to substrate **1** in the absence of free N–SR ligand to drive the equilibrium to the right. The bis-amino species was detectable and proved to be inert (no further reactions were observed). In the presence of free N–SR ligand and activated olefin fn, the formation of the corresponding allylamine species was observed.

As can be seen in Table 1, the rate of nucleophilic attack at the allyl group (k_2) increases with increasing basicity under comparable steric requirements (piperidine is much more reactive than morpholine), this trend being virtually independent of the nature of the allyl group and of the bidentate ligand in the metal substrate. Furthermore, diethylamine and morpholine display roughly the same reactivity despite their different basicity owing to the higher steric demands of the former. Similar behavior was observed in previous studies on related nucleophilic attack at the allyl moiety [1,2]. No marked differences in reactivity can be detected on varying the R group from Ph to *t*-Bu for the same allyl moiety. Apparently, allyl reactivity toward nucleophilic attack is hardly affected by the donor ability of sulfur as governed by the electronic properties of R. Substitution at the 1- and 2-allyl carbons by methyl groups brings about a marked and similar decrease in reactivity, presumably for both electronic and steric reasons. In the case of 1,1-dimethyl allyl substrates a mixture of allylamine products **3** is formed, depending on the relative rates of attack at the two allyl termini as shown by the ^{1}H-NMR spectra (see further). With HY = pip, morph attack at the less substituted carbon is favored in the ratios of 6.4:1 and of 3.1:1, respectively for R = Ph (**1c**) and in the ratios of 2.2 and 1.9 for R = *t*-Bu (**1f**).Apparently the k_2 values determined in these cases are overall constants. As a matter of fact $k_2 = (k_{2m} + k_{2l})$ where k_{2m} and k_{2l} represent the rate constants of amine attack to the more and to the less substituted terminus of the allyl group, respectively. Moreover such ratio equals k_{2l}/k_{2m}, so that in principle it would be possible to determine both constants, were it not for the much higher uncertainties in the ratio values. With HY = dea, only the attack at the less substituted carbon is observed, leading to allylamine **3b**. No interconversion between **3a** and **3b** is observed on the basis of ^{1}H-NMR spectra, at variance with previous findings in analogous systems [9]. The ratios of **3b/3a** observed seem to be in disagreement with an earlier observation [9] that donor ligands induce preferential attack at the less substituted allyl terminus, although the two bidentate ligands under comparison are not highly different as far as overall donor–acceptor properties are concerned. Moreover, the asymmetry of chelate ligand and the fluxional behavior displayed by this class of complexes (Ref. [2] and NMR section in this paper) may affect significantly the regioselectivity of nucleophilic attack, so that the allylamine isomeric ratio turns out to issue from a balance of steric, electronic and dynamic factors which is hard to disentangle.

As could be anticipated, the donor properties of the sulfur substituent come fully into play when affecting

Table 1
Second order rate constants (k_2, mol^{-1} dm^3 s^{-1}) and equilibrium constants (K_E) (Scheme 2) for reactions of allyl complexes with amines at 25°C in $CHCl_3$

Complex		Amine		
		Piperidine	Diethylamine	Morpholine
		pK_a^a 11.12	pK_a 10.84	pK_a 8.50
1a[b]	k_2	3.9 ± 0.3	0.78 ± 0.02	1.19 ± 0.03
	K_E	204 ± 60	69 ± 2	4.1 ± 0.5
1b	k_2	0.106 ± 0.004	(3.3 ± 0.2)10^{-2}	(8.8 ± 0.2)10^{-3}
	K_E	292 ± 32	76 ± 9	2.5 ± 0.2
1c	k_2	0.163 ± 0.002	(2.03 ± 0.08)10^{-2}	(1.5 ± 0.2)10^{-2}
	K_E	18 ± 1	12 ± 2	6 ± 1
1d	k_2	2.75 ± 0.08	0.455 ± 0.006	0.245 ± 0.06
	K_E	3.1 ± 0.4	018 ± 0.01	0.52 ± 0.05
1e	k_2	(8.6 ± 0.4)10^{-2}	(2.93 ± 0.09)10^{-2}	(5.2 ± 0.5)10^{-3}
	K_E	1.4 ± 0.2	1.0 ± 0.1	0.12 ± 0.02
1f	k_2	(9.3 ± 0.3)10^{-2}	(1.3 ± 0.1)10^{-2}	(1.26 ± 0.05)10^{-2}
	K_E	0.6 ± 0.3	0.15 ± 0.03	(5.9 ± 0.7)10^{-2}
1g	k_2	10.0 ± 0.6	2.54 ± 0.05	3.9 ± 0.4
	K_E	2100 ± 200	850 ± 40	42 ± 7

[a] In water.
[b] From Ref. [2].

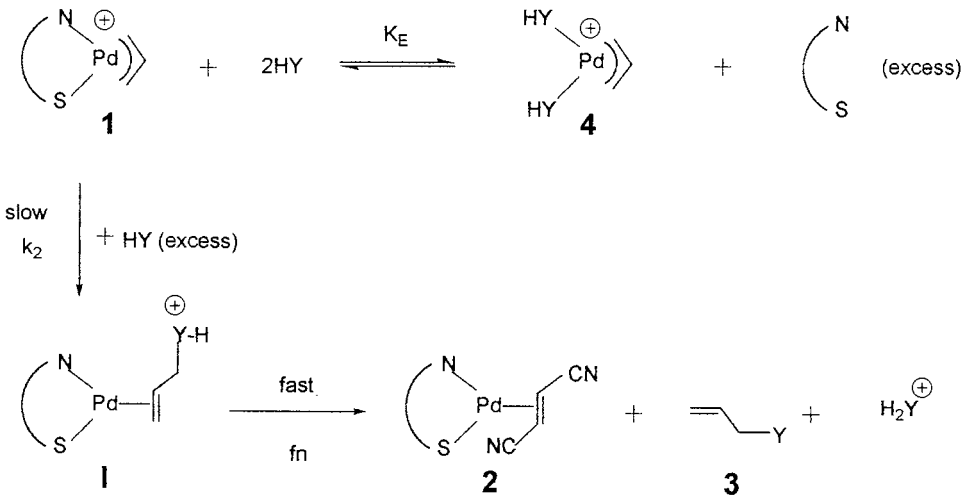

Scheme 2.

the stability of the metal chelate ring. This is reflected by the values of the equilibrium constant K_E pertaining to displacement of N–SR by the entering amine (Table 1, Scheme 1: $K_E = 204 \pm 60$ for **1a**, 3.1 ± 0.4 for **1d**). Consistently, K_E for $[Pd(\eta^3\text{-}C_3H_5)(N–SR)]^+$ (R = Et) is 8.0 ± 0.5 [2]. Increasing substitution at the allyl group brings about an increase in chelate ring stability (i.e. lower K_E values), probably due to increasing steric crowding around the coordination center.

The complex **1g** appears to be the most reactive toward allyl amination (k_2) and bidentate ligand nucleophilic displacement (K_E). The comparatively high k_2 values for the amines investigated (cfr. complex **1a**) would be unexpected on the basis of the higher donor ability of the 6-methyl substituted pyridine ring in **1g** (which should render the allyl group less prone to nucleophilic attack). Therefore, this higher reactivity can probably be traced back to some distorsion of the allyl moiety induced in the ground state which somehow resembles a Pd(0) olefin-like transition state [10]. The high K_E value for **1g** also conflicts with the expected higher stability of the metal–chelate ring due to the higher basicity of pyridine nitrogen, other things being equal. Here, release of steric strain upon displacement by the entering amine around the metal center might be invoked. We sought a kinetics-independent measurement of K_E for **1g** by determining its value directly. Unfortunately, unfavorable spectral changes hampered any attempt in this respect. However, we were able to determine directly by spectrophotometric titration the overall equilibriu-m constant K_{exc} for exchange of bidentate ligand N–SPh (R_3 = Me, Scheme 1) with the α-diimine ligand C_5H_4N-2-CH=NC_6H_4OMe-4 (N–N′) (Eq. 4):

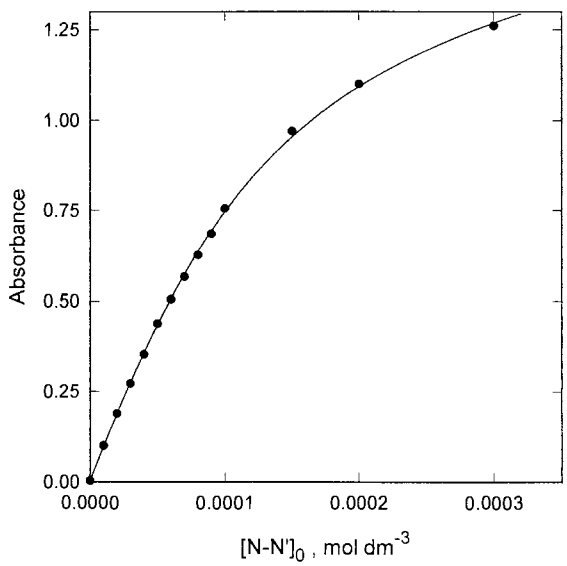

Fig. 2. Fit of absorbance at 400 nm to [N–N′] for the exchange equilibrium on **1g** (Eq. 4; N–N′=C_5H_4N-2-CH=NC_6H_4OMe-4) in $CHCl_3$ at 25°C.

Non linear regression of absorbance data versus [N–N′] according to the model described in Section 5 (Fig. 2) gave a value of 224 ± 25 for K_{exc}, which is in excellent agreement with the average value (253) obtained from the ratios $K_{E(6\text{-MeN–SPh})}/K_{E(N–N')}$ for each amine investigated ($K_{E(L–L')}$ represents the equilibrium constant of displacement of bidentate ligand L–L′ by a given amine. $K_{E(N–N')}$ data were available from our previous work ([1]b). This agreement also confirms the internal consistency of the parameter estimation procedure embodied in the kinetic model of Eq. 3.

The preceding discussion does not take into account the relative role played by all conceivable isomers orig-

$$[Pd(\eta^3\text{-}C_3H_5)(N–SPh)]^+ + N–N' \overset{K_{exc}}{=\!=} [Pd(\eta^3\text{-}C_3H_5)(N–N')]^+ + N–SPh \quad (4)$$

(**1g**) (**5g**)

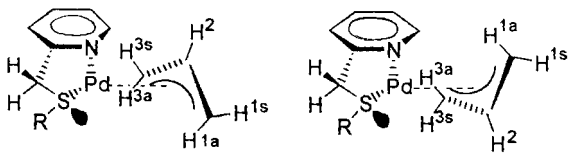

Scheme 3.

inating from the asymmetry of the N–SR ligand, chirality of sulfur, and asymmetry (when present) of the allyl group. In fact, based on NMR results (see further) and on our previous finding [11], we reasonably assume that fluxional interconversion among all such species is fast on the kinetic scale.

3. NMR studies

3.1. Characterisation of complexes **1** and fluxional behavior

The complexes **1a**, **1b**, **1d**, **1e**, and **1g** have the same symmetry and therefore can be grouped together as far as NMR characterisation and behavior are concerned.

In the case of these complexes at low temperature (183 K), we observe only two isomeric forms. Based on our previous findings [2] and those relating to Pd(II) allyl complexes with chelating S-donor ligands ([8]b, [10]), we assign to such isomeric forms the structure of rotational isomers in which the central allyl proton (or methyl group) lies either on the same or on the opposite side as the sulfur substituent with respect to the palladium coordination plane (Scheme 3).

Within these two main structures, each rotational isomer (diastereoisomers D_1, D_2) represents two conformers due to the axial or equatorial position of the sulfur substituent along with their undetectable (under our NMR experimental conditions) enantiomers. The conformers also are undetected, probably owing to the very low conformational barrier which can be easily overcome even at 183 K. Therefore, at low temperature the presence of D_1 and D_2 gives rise to eight distinct signals corresponding to the eight non-equivalent terminal allyl protons (Table 2)

It was not possible to assign these signals to each diastereoisomer D_1 or D_2 by NOE differential spectrometry due to the unfavorable spacial distribution of atoms and the related inter-proton distances [12,13]. Thus, Table 2 lists the signals for each diastereoisomer without commitment of each label (D_1 or D_2) to any species, the D_1 species being assumed to be the more abundant one. On raising the temperature we observe, for each complex, the disappearance of the signals due to the two isomers with concomitant formation of averaged signals ascribable to one species in which four different allyl termini can be distinguished, together with the persistence of an AB quartet ascribed to the S–C$\underline{H}_2$ endocyclic protons. This phenomenon, involving interconversion between diastereoisomers, occurs always at the same temperature independently of solvent and complex concentration and might take place via two main different mechanisms: (i)breaking of the Pd–N bond followed by rotation about the Pd–S bond and reforming of Pd–N bond (apparent allyl rotation via T-shaped intermediate [2,13]); (ii) inversion at sulfur involving exchange of the two coordinating sulfur lone pairs [14]. In both cases the S–C$\underline{H}_2$ protons move into different environments preserving their diastereotopicity because in mechanism (i) sulfur remains a chiral centre and in mechanism (ii) the protons do not mutually exchange with respect to the Pd(η^3-allyl) fragment. This latter mechanism is probably the operative one in our cases, since it is a dissociative, intramolecular rearrangement which is independent of solvent and concentration, as observed, and occurs at lower temperatures than those normally found for 'allyl rotation' [7,10,15]. Moreover, the dissociative nature of the phenomenon rules out a third possible mechanism, i.e. pseudorotation which would require the assistance of some nucleophile (real nucleophiles, counter-ions, impurities, etc.) [16].On further raising of the temperature, other concomitant fluxional phenomena take place. Breaking of Pd–S bonds or pseudo-rotation might become operative, thereby further reducing the terminal allyl proton

Table 2
Selected allyl proton ^{1}H-NMR signals[a]

	1b	1d	1e	1g
H^s (D_1)[b]	4.17(s)	Obscured	4.04(s)	Obscured
	Obscured	4.68(d) (J = 6.8)	Obscured	4.98(d) (J = 7.3)
H^s (D_2)[c]	4.01(s)	Obscured	3.99(s)	4.25(d) (J = 7.2)
	Obscured	4.59(d) (J = 7.3)	Obscured	5.05(d) (J = 7.0)
H^2 (D_2)		5.87(m)		5.80(m)
H^2 (D_2)		5.87(m)		5.80(m)
CH_3 (D_1)	2.16(s)		2.11(s)	
CH_3 (D_2)	2.16(s)		2.13(s)	
H^a (D_1)	2.98(s)	3.05(d) (J = 12.7)	2.89(s)	3.30(d) (J = 12.4)
	3.80(s)	3.92(d) (J = 12.9)	3.73(s)	3.83(d) (J = 13.0)
H^a (D_2)	3.15(s)	3.16(d) (J = 12.8)	3.01(s)	3.45(d) (J = 12.6)
	3.80(s)	3.92(d) (J = 12.9)	3.75(s)	3.86(d) (J = 13.3)
$R = D_1/D_2$	2.1	1.2	1.4	1.8

[a] In CD_2Cl_2 solution at 193 K. δ values are in ppm and J values in Hz.
[b] More and [c] less abundant isomer.

signals to two with companion loss of diastereotopicity of S–C$\underline{H}_2$ protons and collapse of the AB quartet into a singlet. This results in an increased molecular symmetry leading to one single broad signal for *syn* and *anti* protons. Whatever the pathway involved, this process turns out to be affected by the solvent, the complex concentration, and the presence of adventitious impurities, thereby confirming its associative nature.

No evidence of η^3-η^1-η^3 isomerism could be gathered in the temperature range of the present study, except for complex **1a** for which incipient onset of such phenomenon could be detected at comparatively high temperature [2]. For illustration purposes, the ^{1}H-NMR spectra of complexes **1d** at selected temperatures in CD_2Cl_2 are shown in Fig. 3.

In the case of complexes **1c** and **1f**, the four different isomers shown in Scheme 4 can exist.

Since the fluxional behavior of such complexes is the same as the previously described species, we expected the presence of signals indicating four different isomers in the low temperature ^{1}H-NMR spectra, but as can be seen in Fig. 4 relating to **1f**, it is not possible to detect all the signals arising from the four different isomers even at -90°C. Only the four signals of methyl protons of the *t*-Bu substituent can be easily observed. However, apparent rotation or sulfur inversion become evident at 298 K, where the halving of *t*-Bu signals is accompanied by a marked simplification of the spectral pattern in which only two species can be discerned.

In Section 5 we report for instance the proton chemical shifts corresponding to such a situation, wherein each pair (**a**, **d)** and (**b**, **c)** would behave as one single species if mechanism (i) was operative ((**a**, **b)** and (**c**, **d)** in the case of mechanism (ii)). In fact, apparent rotation or the more likely sulfur inversion will reduce the total number of diastereoisomers from four to two. Again, loss of sulfur chirality can be observed on further increasing the temperature, due to the concomitant occurrence of more than one phenomenon.

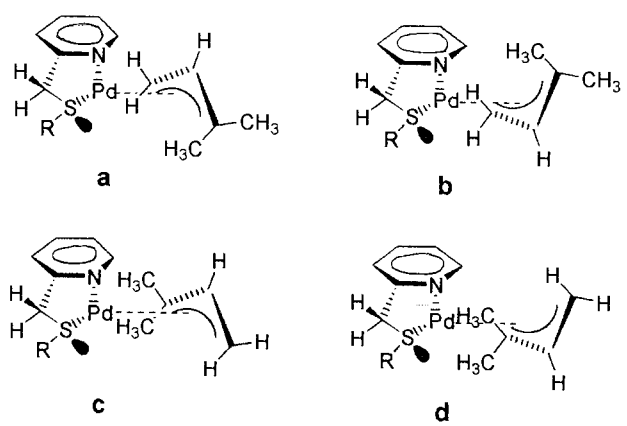

Scheme 4.

At the highest temperature achieved in $C_2D_2Cl_4$, only the signals pertaining to one single species are detected, with distinct *syn* and *anti* protons and *syn* and *anti* methyl groups. As a matter of fact, the incipient simplification of the central H^2 allyl proton signals would suggest the occurrence of the η^3-η^1-η^3 isomeric mechanism.

3.2. Allyl amination reactions

All the reactions that were studied by UV–VIS spectrophotometric techniques were also examined by ^{1}H-NMR spectrometry. In any case, formation of Pd(0) complexes **2a**, **2d**, and **2g** and the corresponding allylamine species was confirmed when the starting metal substrates **1(a–c)**, **1(d–f)**, and **1g** were reacted with amines in the presence of fumaronitrile. The addition of amine will induce a generalized fluxionality on the starting complexes. Since we recently determined [2,11] that the change of sulfur absolute configuration in this type of complex is associative, leading to loss of diastereotopicity of C$\underline{H}_2$–S protons, and because the presence of amine lowers the temperature at which this phenomenon takes place, we are led to conclude that the presence of a nucleophile may frustrate any attempt at a designed synthesis based on electronic effects. No further information can be gathered from the system under these experimental conditions. As a matter of fact, analysis of the ^{1}H-NMR spectra does not allow us to confirm such mechanistic paths as being breaking and re-forming of the Pd–N bond or even Berry's pseudorotation, which might also be operative under these conditions.

4. Conclusions

From the kinetic data of this work (Eq. 2) and previous evidence [1,2] we conclude that when good nucleophiles toward Pd(II) are used for nucleophilic attack at the coordinated allyl moiety, an overall decrease in rate is observed due to extensive displacement of the bidentate ligand by the nucleophile, especially in the presence of ancillary ligands bearing poor coordinating atoms such as nitrogen or sulfur. On the other hand, strong donors like phosphorus appear to promote fluxionality as well as inducing η^3-η^1-η^3 isomerism [7,15,17,18], thanks to their high *trans* influence. Steric factors may be the key features in the allylamine synthesis, although no generalization is warranted. As a matter of fact, increased steric requirements would depress the rates of allyl amination, thereby favoring other side reactions, such as formation of trace amounts of isoprene via allyl deprotonation, as observed in the case of **1c**, **1f**, or other complexes [19] reacting with diethylamine.

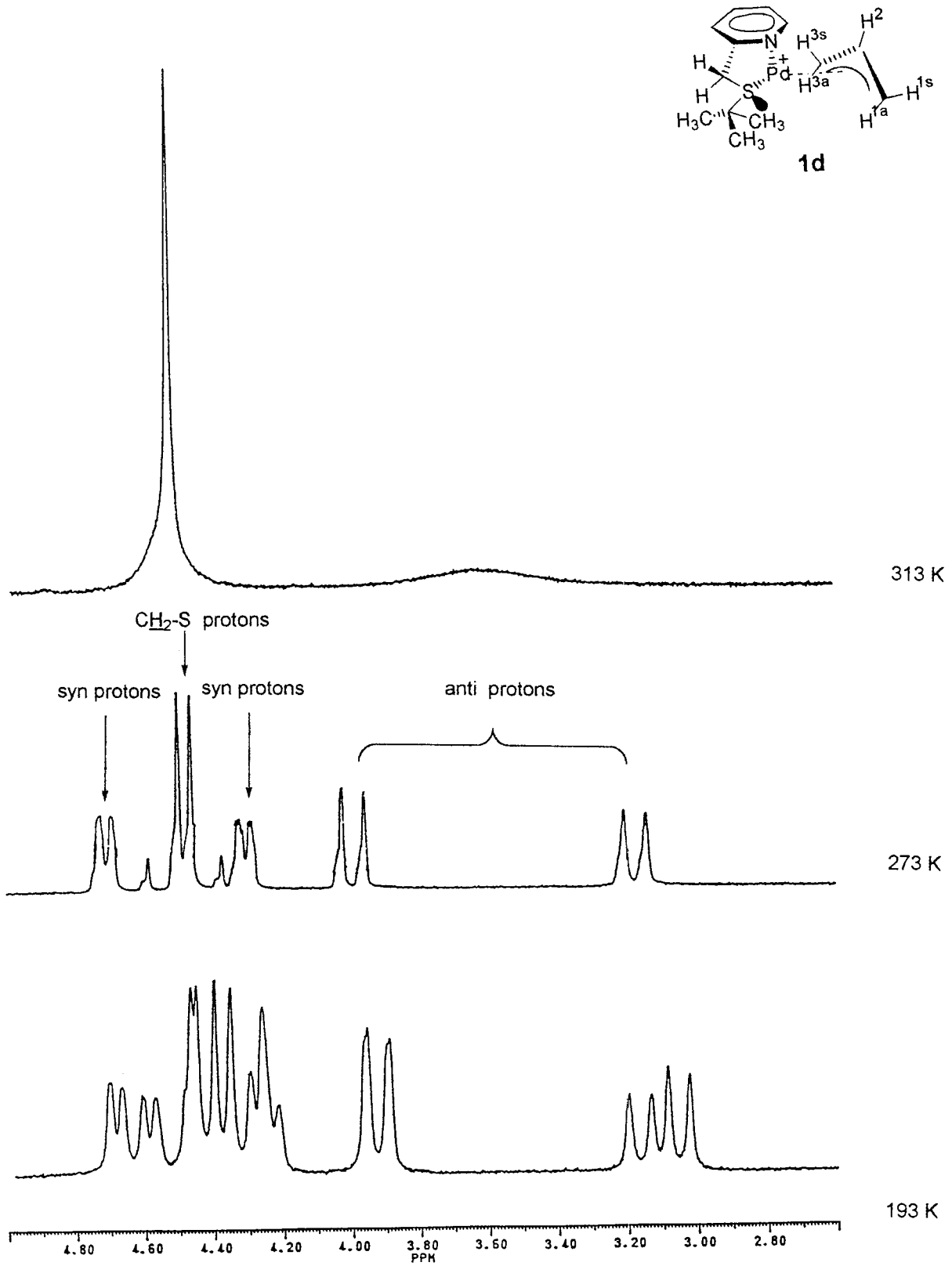

Fig. 3. Selected region of ^{1}H-NMR spectra of **1d** at various temperatures in CD_2Cl_2 at 200 MHz. Representation on the top of the figure implies no isomeric preference.

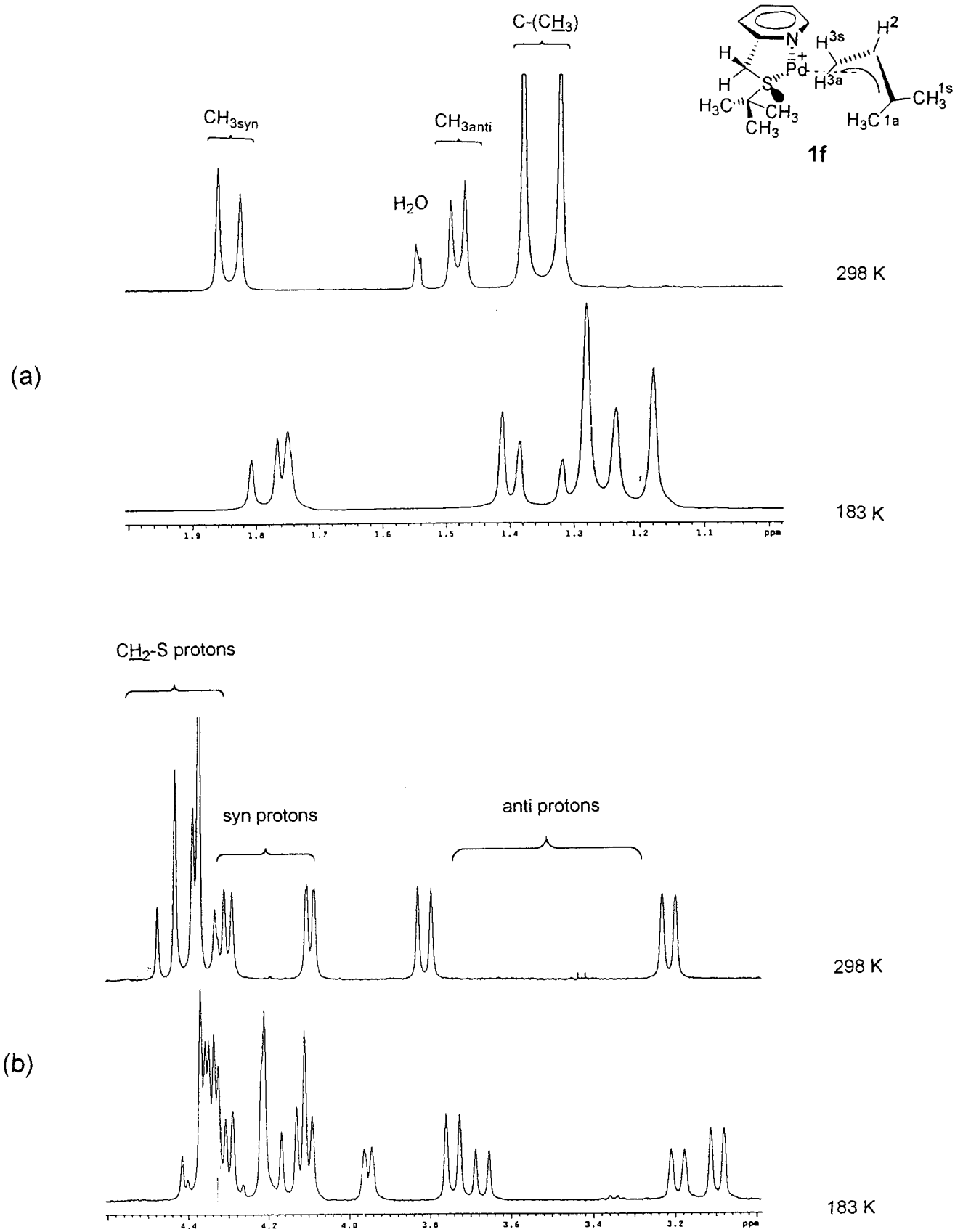

Fig. 4. Selected regions (methyl groups (a) and allyl and C$\underline{H}_2$–S protons (b)) of ^{1}H-NMR spectra of **1f** at different temperatures in CD_2Cl_2. Representation on the top of the figure implies no isomeric preference

5. Experimental

5.1. Preparation of ligands

5.1.1. 2-Chloromethyl-6-methylpyridine

This ligand was synthesized as in Ref. [20]. Yield 92%.^{1}H-NMR ($CDCl_3$): $\delta_{(ppm)}$ 2.51 (–C$\underline{H}_3$: s, 3H); 4.59 (C$\underline{H}_2$–Cl: s, 2H); 7.04 ($H^3_{(pyr)}$: d, $J = 7.7$, 1H); 7.22 ($H^5_{(pyr)}$: d, $J = 7.7$, 1H); 7.55 ($H^4_{(pyr)}$: t, $J = 7.7$, 1H). ^{13}C-NMR ($CDCl_3$): $\delta_{(ppm)}$ 24.3; 46.8; 119.7; 122.6; 137.2; 155.8; 158.2. IR: $\nu_{(CN)}$ 1595 cm^{-1} (NaCl windows).

5.1.2. 2-(Phenylthiomethyl)pyridine

This ligand was synthesized as in Ref. [2]. Yield 80%. ^{1}H-NMR ($CDCl_3$): $\delta_{(ppm)}$ 4.70 (C$\underline{H}_2$–S: s, 2H); 7.60 ($H^4_{(pyr)}$: t, $J = 7.7$, 1H); 8.58 ($H^6_{(pyr)}$,: d, $J = 4.7$, 1H). ^{13}C-NMR ($CDCl_3$): $\delta_{(ppm)}$ 40.2; 121.7; 122.6; 126.0; 128.6; 129.2; 135.6; 136.2;149.0; 157.4. IR: $\nu_{(CN)}$ 1616 cm^{-1} (as hydrochloride, KBr pellet).

5.1.3. 2-Phenylthiomethyl-6-methylpyridine

To a stirred suspension of powdered KOH (6.73 g, 120 mmol) in dry DMSO (30 cm^3) containing thiophenol (3.3 g, 30 mmol) was added 2-chloromethyl-6-methylpyridine (2.12 g, 15 mmol). Stirring was continued for 1 h at 25°C then water (50 cm^3) was added and the product was extracted with diethyl ether (2×50 cm^3). The organic extract was washed with water, dried (Na_2SO_4) and concentrated to yield a residue which was flash chromatographed (SiO_2) eluting with 10% ethyl acetate in hexane elution to give an oil (2.92 g, 96%). ^{1}H-NMR ($CDCl_3$): $\delta_{(ppm)}$ 2.52 (–C$\underline{H}_3$: s, 3H); 4.23 (C$\underline{H}_2$–S: s, 2H); 7.15 ($H^{3,5}_{(pyr)} + H_{(phen)}$: m, 7H); 7.44 ($H^4_{(pyr)}$: t, $J = 7.6$,1H). ^{13}C-NMR ($CDCl_3$): $\delta_{(ppm)}$ 24.4; 40.4; 119.8; 121.6; 126.1; 128.8; 129.4; 136.1; 136.8; 156.8; 158. IR: $\nu_{(CN)}$ 1591 cm^{-1}(NaCl windows).

5.1.4. 2-(tert-Butylthiomethyl)pyridine

The title compound was prepared from 2-methyl-2-propanethiol (1.17 g, 13 mmol) and 2-picolylchloride hydrochloride (1.07 g, 6.5 mmol) in DMSO (15 cm^3) in the presence of KOH (2.91 g, 52 mmol) using the procedure described above for 2-phenylthiomethyl-6-methylpyridine. Purification by flash chromatography (SiO_2) by elution first with CH_2Cl_2 then with 10% diethyl ether in CH_2Cl_2 yielded the required thioether as an oil (1.42 g, 81%). ^{1}H-NMR($CDCl_3$): $\delta_{(ppm)}$ 1.31 (C–C$\underline{H}_3$: s, 9H); 3.89 (C$\underline{H}_2$–S: s, 2H); 7.09 (H^5:m, 1H); 7.38 ($H^3_{(pyr)}$:d, $J = 7.8$, 1H); 7.59 ($H^4_{(pyr)}$: t, $J = 7.8$, 1H); 8.48 ($H^6_{(pyr)}$: d, $J = 5.4$, 1H). ^{13}C-NMR ($CDCl_3$): $\delta_{(ppm)}$ 30.9; 35.6; 43.0; 121.6; 123.2; 136.4; 149.1; 159.1. IR $\nu_{(CN)}$ 1591 cm^{-1}(NaCl windows).

5.2. Preparation of Pd(II) complexes

5.2.1. [Pd(η^3-C_3H_5)(C_5H_4N-2-$CH_2SC(CH_3)_3$)]ClO_4 (1d)

To a solution of [Pd(η^3-C_3H_5)Cl]$_2$ (0.185 g, 0.505 mmol) in CH_2Cl_2 (25 cm^3), 2-(*tert*-butylthiomethyl)pyridine (0.183 g, 1.01 mmol) dissolved in CH_2Cl_2 (5 cm^3) were added. To the stirred mixture addition of $NaClO_4$ (0.287 g, 2.04 mmol) in MeOH (10 cm^3) yielded the precipitation of NaCl with concomitant decoloration of the solution. The reaction mixture was stirred for 0.5 h and the solvent removed under reduced pressure. The resulting sticky solid was dissolved in CH_2Cl_2 (20 cm^3), treated with activated charcoal and filtered on celite. The resulting clear solution, concentrated under reduced pressure, yielded the crude product **1d** as an off-white solid upon addition of diethyl ether. The crude product was recrystallized from CH_2Cl_2/diethyl ether (0.414 g, 96%). Found: C 36.51; H 4.80; N 3.31; S 7.45. $C_{13}H_{20}NSO_4ClPd$ requires C 36.46; H 4.71; N 3.27; S 7.49%.IR: $\nu_{(CN)}$ 1603; $\nu_{(ClO)}$ 1092; $\delta_{(ClO)}$ 623 cm^{-1} (KBr pellet). ^{1}H-NMR (CD_2Cl_2 193 K): $\delta_{(ppm)}$ 1.37 (D_1, C–(C$\underline{H}_3$)$_3$: s), 1.26 (D_2, C–(C$\underline{H}_3$)$_3$: s);4.30 ($D_1 + D_2$, C$\underline{H}_2$–S: m (two mixed AB systems)); 7.44 ($D_1 + D_2$, $H^5_{(pyr)}$: m); 7.77 ($D_1 + D_2$,$H^3_{(pyr)}$: d, $J = 7.8$); 8.00 ($D_1 + D_2$,$H^4_{(pyr)}$: t, $J = 7.8$); 8.72 ($D_1 + D_2$,$H^6_{(pyr)}$: m); allyl signals: see Table 2.

5.2.2. [Pd(η^3-C_3H_5)(C_5H_4N-2-$CH_2SC_6H_5$)]ClO_4 (1a)

This complex was prepared as in Ref. [2]. Yield 89% (white microcrystals). Found: C 40.15; H 3.51; N 3.00; S 6.81. $C_{15}H_{16}NSO_4ClPd$ requires C 40.19; H 3.60; N 3.12; S 7.15%. IR: ν_{CN} 1603; ν_{ClO} 1088; δ (ClO) 623 cm^{-1} (Nujol mull). ^{1}H-NMR (CD_2Cl_2 193 K): $\delta_{(ppm)}$ 4.56,4.64, (D_1, C$\underline{H}_2$–S AB sys. $J = 16.8$); 4.48, 4.96, (D_2, C$\underline{H}_2$–S AB sys. $J = 16.7$); 7.45 ($D_1 + D_2$, $H^{3,3'}_{(phen)}$: d, $J = 8.1$); 7.59 ($D_1 + D_2$, $H^{2,2'}_{(phen)}$ d, $J = 8.1$); 7.29–7.39 ($D_1 + D_2$,$H^4_{(phen)} + H^5_{(pyr)}$: m); 7.62 ($D_1 + D_2$, $H^3_{(pyr)}$: d, $J = 7.9$); 7.95 ($D_1 + D_2$, $H^4_{(pyr)}$: t, $J = 7.9$); 8.80 (D_1,$H^6_{(pyr)}$: d, $J = 4.6$); 8.78 (D_2,$H^6_{(pyr)}$: d, $J = 5.6$); allyl signals: see Ref. [2].

Complexes **1b**, **1c**, **1e**, **1f**, and **1g** were synthesized as **1d** complex using the appropriate pyridine–thioether.

5.2.3. [Pd(η^3-2-MeC_3H_4)(C_5H_4N-2-CH_2 SC_6H_5)]ClO_4 (1b)

Yield 85% (white microcrystals). Found: C 42.02; H 3.85; N 3.11; S 7.01. $C_{16}H_{18}NSO_4ClPd$ requires C 41.57; H 3.92; N 3.03; S 6.94%. IR: $\nu_{(CN)}$ 1599; $\nu_{(ClO)}$ 1088; $\delta_{(ClO)}$ 623 cm^{-1} (KBr pellet). ^{1}H-NMR (CD_2Cl_2 193 K): $\delta_{(ppm)}$ 4.63 ($D_1 + D_2$,C$\underline{H}_2$–S: m (two mixed AB systems)); 7.50 ($D_1 + D_2$,$H_{(phen)} + H^5_{(pyr)} + H^3_{(pyr)}$: m); 7.97 ($D_1 + D_2$, $H^4_{(pyr)}$: t, $J = 7.8$); 8.81 ($D_1 + D_2$,$H^6_{(pyr)}$: d, $J = 5.2$); allyl signals: see Table 2.

*5.2.4. [Pd(η³-1,1-$Me_2C_3H_3$)(C_5H_4N-2-$CH_2SC_6H_5$)]ClO_4 (**1c**)*

Yield 87% (white microcrystals). Found: C 43.01; H 4.18; N 3.03; S 6.81. $C_{17}H_{20}NSO_4ClPd$ requires C 42.87; H 4.23; N 2.94; S 6.73%. IR: $\nu_{(CN)}$ 1606; $\nu_{(ClO)}$ 1103: $\delta_{(ClO)}$ 623 cm^{-1} (KBr pellet). ^{1}H-NMR (CD_2Cl_2 298 K): $\delta_{(ppm)}$ 1.29 (D_1,CH_{3anti}: bs), 1.54 (D_2,CH_{3anti}: bs); 1.67 (D_1,CH_{3syn}: bs), 1.83 (D_2,CH_{3syn}: bs); 3.92 (D_1, H_{anti}: bs), 3.37 (D_2, H_{anti}: bs); 4.45 (D_1, H_{syn}: bs),4.20 (D_2, H_{syn}: bs); 4.70 (D_1+D_2,C$\underline{H}_2$–S:bs); 5.63 (D_1+D_2, $H^2_{(allyl)}$: bs); 7.38–7.55 (D_1+D_2,$H_{(phen)}+H^5_{(pyr)}$: m); 7.63 (D_1+D_2, $H^3_{(pyr)}$: d, $J=7.8$); 7.98 (D_1+D_2, $H^4_{(pyr)}$: t, $J=7.8$); 8.84 (D_1, $H^6_{(pyr)}$: bs); 8.55 (D_2, $H^6_{(pyr)}$: bs).

*5.2.5. [Pd(η³-2-MeC_3H_4)(C_5H_4N-2-$CH_2SC(CH_3)_3$)]ClO_4 (**1e**)*

Yield 92% (white microcrystals). Found: C 38.13; H 4.95; N 3.22; S 7.30. $C_{14}H_{22}NSO_4ClPd$ requires C 38.02; H 5.01; N 3.17; S 7.25%. IR: $\nu_{(CN)}$ 1603; $\nu_{(ClO)}$ 1090; $\delta_{(ClO)}$ 623 cm^{-1} (KBr pellet). ^{1}H-NMR (CD_2Cl_2 193 K): $\delta_{(ppm)}$1.36 (D_1,C–(C$\underline{H}_3$)$_3$: s); 1.29 (D_2,C–(C$\underline{H}_3$)$_3$: s); 4.39, (D_1+D_2, C$\underline{H}_2$–S (two mixed AB systems): m); 7.44 (D_1+D_2, $H^5_{(pyr)}$: m); 7.77 (D_1+D_2, $H^3_{(pyr)}$: d, $J=7.8$); 8.00 (D_1+D_2,$H^4_{(pyr)}$: t, $J=7.8$); 8.73 (D_1+D_2,$H^6_{(pyr)}$: d, $J=5.2$); allyl signals: see Table 2.

*5.2.6. [Pd(η³-1,1-$Me_2C_3H_3$)(C_5H_4N-2-$CH_2SC(CH_3)_3$)]ClO_4 (**1f**)*

Yield 97% (white microcrystals). Found: C 39.75; H 5.35; N 3.15; S 7.09. $C_{15}H_{24}NSO_4ClPd$ requires C 39.48; H 5.30; N 3.07; S 7.03%. IR: $\nu_{(CN)}$ 1603; $\nu_{(ClO)}$ 1090; $\delta_{(ClO)}$ 623 cm^{-1} (KBr pellet). ^{1}H'-NMR (CD_2Cl_2 298 K): $\delta_{(ppm)}$ 1.38 (D_1,C–(C$\underline{H}_3$)$_3$: s), 1.32 (D_2, C–(C$\underline{H}_3$)$_3$: s); 1.47 (D_1, CH_{3anti}: s), 1.49 (D_2,CH_{3anti}: s); 1.86 (D_1, CH_{3syn}: s); 1.83 (D_2, CH_{3syn}: s); 3.82 (D_1, H_{anti}: d, $J=13.6$), 3.22 (D_2, H_{anti}: d, $J=2.7$); 4.10 (D_1, H_{syn}: d, $J=7.5$), 4.30 (D_2, H_{syn}: d, $J=7.9$); 4.40, (D_1+D_2, C$\underline{H}_2$–S (two mixed AB systems): m); 5.41 (D_1, $H^2_{(allyl)}$: d,d, $J=13.6,7.5$), 5.64 (D_2 $H^2_{(allyl)}$: d,d, $J=12.7,7.9$); 7.58 (D_1,$H^5_{(pyr)}$: d,d, $J=7.9$, 5.3),7.45 (D_2,$H^5_{(pyr)}$: d,d, $J=7.9$, 4.8); 7.82 (D_1, $H^3_{(pyr)}$: d, $J=7.9$); 7.75 (D_2, $H^3_{(pyr)}$: d, $J=7.9$); 8.05 (D_1,$H^4_{(pyr)}$: t, $J=7.9$); 7.99 (D_2,$H^4_{(pyr)}$: t, $J=7.9$); 8.45 (D_1, $H^6_{(pyr)}$: d, $J=5.3$); 8.74 (D_2, $H^6_{(pyr)}$: d, $J=4.8$).

*5.2.7. [Pd(η³-C_3H_5)(C_5H_3N-6-Me-2-CH_2 SC_6H_5)]ClO_4 (**1g**)*

Yield 92% (white microcrystals). Found: C 41.71; H 4.01; N 3.08; S 6.98. $C_{16}H_{18}NSO_4ClPd$ requires C 41.57; H 3.92; N 3.03; S 6.94%. IR: $\nu_{(CN)}$ 1603; $\nu_{(ClO)}$ 1086; $\delta_{(ClO)}$ 625 cm^{-1} (KBr pellet). ^{1}H-NMR (CD_2Cl_2 193 K): $\delta_{(ppm)}$ 2.76 (D_1, –C$\underline{H}_3$: s), 2.72 (D_2, –C$\underline{H}_3$: s); 4.73, (D_1+D_2, C$\underline{H}_2$–S (two mixed AB systems): m); 7.45 (D_1+D_2, $H_{(phen)}+H^5_{(pyr)}+H^3_{(pyr)}$: m); 7.77 ($D_1+D_2$, $H^4_{(pyr)}$: t, $J=7.4$); allyl signals: see Table 2.

5.3. Preparation of Pd(0) complexes

*5.3.1. [Pd(η²-$(CHCN)_2$)(C_5H_4N-2-$CH_2SC(CH_3)_3$)] (**2d**)*

To a solution of (2-(*tert*-butylthiomethyl)pyridine) (0.083 g, 0.46 mmol) in anhydrous acetone (10 cm^3), Pd_2DBA_3C $CHCl_3$ (0.215 g, 0.21 mmol) and fn (0.0357 g, 0.45 mmol) were added under nitrogen. The initial dark suspension of reagents slowly dissolved (1.5 h) giving a yellowish solution. Addition of activated charcoal and filtration on celite removed metallic palladium yielding a bright yellow solution. Reduction to small volume (3–4 cm^3) and addition of diethyl ether (15 cm^3) gave a pale yellowish precipitate which was filtered off and washed with diethyl ether in excess to remove the DBA (the resulting washing solvent was colorless). The microcrystals were dried under reduced pressure and stored under inert atmosphere (0.127 g, 87%). Found: C 45.85; H 4.61; N 11.52; S 8.91. $C_{14}H_{17}N_3SPd$ requires C 45.97; H 4.68; N 11.49; S 8.76%. IR:$\nu_{(CN)}$ 2195 (fn): $\nu_{(CN)}$ 1597 (pyridine ring) cm^{-1} (KBr pellet). ^{1}H-NMR ($CDCl_3$ 298 K): δ 1.49 (C–(C$\underline{H}_3$)$_3$: s, 9H); 3.10 (olefin protons: br. AB system, 2H); 4.21 (C$\underline{H}_2$–S: s, 2H); 7.35 ($H^5_{(pyr)}$: m,1H); 7.51 ($H^3_{(pyr)}$: d, $J=7.5$, 1H); 7.84 ($H^4_{(pyr)}$: t, $J=7.5$,1H); 8.90 ($H^6_{(pyr)}$: d, $J=6.0$,1H).

Complex **2g** was prepared as **2d**.

*5.3.2. [Pd(η²-$(CHCN)_2$)(C_5H_3N-6-Me-2-$CH_2SC_6H_5$)] (**2g**)*

Yield 82% (pale yellow microcristals). Found: C 51.13; H 3.84; N 10.43; S 8.12. $C_{17}H_{15}N_3SPd$ requires C 51.07; H 3.78; N 10.51; S 8.02%. IR: $\nu_{(CN)}$ 2200 (fn): $\nu_{(CN)}$ 1602 (pyridine ring) cm^{-1} (KBr pellet). ^{1}H-NMR ($CDCl_3$ 298 K): $\delta_{(ppm)}$ 2.93 (–C$\underline{H}_3$: s, 3H); 3.18 (olefin proton: bs, 2H); 4.51 (C$\underline{H}_2$–S: s, 2H); 7.40 ($H^3_{(pyr)}+H^5_{(pyr)}+H_{(phen)}$: m, 7H); 7.67 ($H^4_{(pyr)}$: t, $J=7.7$, 1H).

Complex **2a** was prepared as in Ref. [2].

*5.3.3. [Pd(η²-$(CHCN)_2$(C_5H_4N-2-$CH_2SC_6H_5$)) (**2a**)*

Yield 78% (pale yellow microcrystals). Found: C 49.99; H 3.41; N 10.86; S 8.16. $C_{16}H_{13}N_3SPd$ requires C 49.82; H 3.40; N 10.89; S 8.31%. IR: $\nu_{(CN)}$ 2199 (fn): $\nu_{(CN)}$ 1601 (pyridine ring) cm^{-1} (Nujol mull). ^{1}H-NMR ($CDCl_3$ 298 K): $\delta_{(ppm)}$ 3.21 (olefin proton: bs, 2H); 4.48 (C$\underline{H}_2$–S: bs, 2H); 7.51 ($H^3_{(pyr)}+H^5_{(pyr)}+H^6_{(pyr)}+H_{(phen)}$: m, 7H); 7.82 ($H^4_{(pyr)}$: t, $J=7.7$, 1H); 8.95 ($H^6_{(pyr)}$: d, $J=5.0$,1H).

5.4. Spectrophotomeric studies

The kinetics of allyl amination of complexes **1** were studied by adding known aliquots of amine solution to a solution of **1**, fn and the appropriate ligand N–SR in the thermostatted cell compartment of the spectrophotometer. The reactants were such to ensure constant excess over the metal complex ($[Pd]_0$ ca. 1×10^{-4} mol dm^{-3}). The progress of the reaction was monitored by

recording absorbance changes either in the range 300–500 nm or at fixed wavelength with time.

The overall equilibrium constant K_{exc} for the bidentate ligand exchange (Eq. 4) was determined as follows: to a solution of **1g** (1×10^{-4} mol dm^{-3}) and N–SPh (R_3 = Me, Scheme 1) (9.786×10^{-3} mol dm^{-3}) in 100 cm^3 of $CHCl_3$ successive microaliquots of α-diimine C_5H_4N-2-CH=NC_6H_4OMe-4 (N–N′) were added. After each addition, 3 cm^3 of the resulting solution were placed in the thermostatted (25°C) spectrophotometric cell compartment and the UV–VIS spectrum in the wavelength range 300–500 nm was recorded. The analytical N–N′ concentration was in the range 1×10^{-5}–3×10^{-4} mol dm^{-3}. Absorbance data at the given wavelength, A_λ, were analyzed as a function of $[N–N']_0$ according to the following model:

$$[N–SPh]\,[\mathbf{5g}]/[N–N']\,[\mathbf{1g}] = K_{exc}$$

$$[\mathbf{1g}] + [\mathbf{5g}] = [Pd]_0$$

$$[N–N'] + [N–SPh] = [N–N']_0 + [N–SPh]_0$$

$$[N–SPh] = [N–SPh]_0 + [\mathbf{5g}]$$

$$A_\lambda = \varepsilon_{1g}[\mathbf{1g}] + \varepsilon_{5g}[\mathbf{5g}] + \varepsilon_{N–SPh}[N–SPh] + \varepsilon_{N–N'}[N–N']$$

Non-linear regression of absorbance data was carried out as described earlier ([1]b).

5.5. Instrumentation and data analysis

IR spectra were obtained with a Nicolet Magna IR 750, UV–VIS spectra on a Perkin–Elmer lambda 5, ^{1}H and ^{13}C-NMR spectra with Bruker AC 200 and Varian Unity 400 spectrometers. Mathematical and statistical data analysis was carried out on a personal computer by means of a locally adapted version of Marquardt's algorithm [21] written in TURBOBASIC™ (Borland).

Acknowledgements

Financial support by the Italian Ministero dell'Universita' e della Ricerca Scientifica e Tecnologica and the University of Venice is gratefully acknowledged. We also thank Lucia Gemelli for her technical assistance.

References

[1] (a) B. Crociani, S. Antonaroli, F. Di Bianca, L. Canovese, F. Visentin, P. Uguagliati, J. Chem. Soc. Dalton Trans. (1994) 1145. (b) L. Canovese, F. Visentin, P. Uguagliati, F. Di Bianca, S. Antonaroli, B. Crociani, J. Chem. Soc. Dalton Trans. (1994) 3113. (c) L. Canovese, F. Visentin, P. Uguagliati, B. Crociani, F. Di Bianca, Inorg. Chim. Acta 235 (1995) 45. (d) L. Canovese, F. Visentin, P. Uguagliati, F. Di Bianca, A. Fontana, B. Crociani, J. Organomet. Chem. 508 (1996) 101.
[2] L. Canovese, F. Visentin, P. Uguagliati, G. Chessa, V. Lucchini, G. Bandoli, Inorg. Chim. Acta 275 (1998) 385.
[3] (a) J. Tsuji, Palladium Reagents and Catalysts, Wiley, Chichester, UK, 1995, Ch. 4.2. (b) B.M. Trost, D.L. Van Vranken, Chem. Rev. 96 (1996) 395.
[4] A. Togni, L.M. Venanzi, Angew. Chem. Int. Ed. Engl. 33 (1994) 497 and references therein.
[5] (a) J. Sprinz, M. Kiefer, G. Helmchen et al., Tetrahedron Lett. 35 (1994) 1523. (b) N. Baltzer, L. Macko, S. Schaffner, M. Zehunder, Helv. Chim. Acta 79 (1996) 803. (c) H.A. Ankersmit, B.H. Loken, H. Kooijman, A.L. Spek, K. Vrieze, G. van Koten, Inorg. Chim. Acta 252 (1996) 141. (d) U. Burckhardt, M. Bauman, A. Togni, Tetrahedron Asymmetry 8 (1997) 155.
[6] S. Mecking, W. Keim, Organometallics 15 (1996) 2650.
[7] A. Albinati, P.S. Pregosin, K. Wick, Organometallics 15 (1996) 2419 and references therein.
[8] (a) C.G. Frost, J.M.J. Williams, Tetrahedron Lett. 34 (1993) 2015. (b) H.A. Ankersmit, N. Veldman, A.L. Speck, K. Eriksen, K. Goubitz, K. Vrieze, G. van Koten, Inorg. Chim. Acta 252 (1996) 203.
[9] B. Åkermark, K. Zetterberg, S. Hansson, B. Krakenberger, A. Vitagliano, J. Organomet. Chem. 335 (1987) 133.
[10] J. Hermann, P.S. Pregosin, R. Salzmann, A. Albinati, Organometallics 14 (1995) 3311.
[11] L. Canovese, F. Visentin, P. Uguagliati, V. Lucchini, G. Bandoli, Inorg. Chim. Acta 277 (1998) 247.
[12] P.S. Pregosin, C.J. Ammann, Pure Appl. Chem. 61 (1989) 1771.
[13] A. Albinati, R.W. Kunz, C.J. Ammann, P.S. Pregosin, Organometallics 10 (1991) 1800.
[14] (a) E.W. Abel, J.C. Dormer, D. Ellis et al., J. Chem. Soc. Dalton Trans. (1992) 1073. (b) S.Y. Chooi, T.T. Andy Hor, P. Leung, K.F. Mok, Inorg. Chem. 31 (1992) 1494. (c) G.R. Giesbrecht, G.S. Hanan, J.E. Kickham, S.L. Loeb, Inorg. Chem. 31 (1992) 3286. (d) E.W. Abel, D. Ellis, K.G. Orrell, V. Sik, J. Chem. Soc. Dalton Trans. (1992) 3497. (e) E.W. Abel, T.P.J. Coston, K.M. Higgins et al., J. Chem. Soc. Dalton Trans. (1989) 701. (f) E.W. Abel, I. Moss, K.G. Orrell et al., J. Chem. Soc. Dalton Trans. (1988) 521.
[15] C. Breutel, P.S. Pregosin, R. Salzmann, A. Togni, J. Am. Chem. Soc. 116 (1994) 4067.
[16] B. Crociani, S. Antonaroli, M. Paci, F. Di Bianca, L. Canovese, Organometallics 16 (1997) 384.
[17] T. Hosokawa, Y. Wakabayashi, K. Hosokawa, T. Tsuji, S.I. Murahashi, J. Chem. Soc. Chem. Commun. (1996) 859.
[18] R. Fernandez-Galan, F.A. Jalon, B.R. Manzano, et al., Organometallics 16 (1997) 3758.
[19] B. Crociani, L. Canovese, unpublished results.
[20] W. Baker, K.M. Buggle, J.F.W. Mc Onic, D.A.M. Watkins, J. Chem. Soc. (1958) 3594.
[21] D.W. Marquardt, SIAM J. Appl. Math. 11 (1963) 431.